Digest Journal of Nanomaterials and Biostructures Vol. 6, No 3, July-September 2011, p. 1367-1376

PARTICLE SIZE AND CONCENTRATION DEPENDENT CYTOTOXICITY OF CITRATE CAPPED GOLD NANOPARTICLES

ANA VUJAČIĆ, VESNA VODNIK, GORDANA JOKSIĆ, SANDRA PETROVIĆ, ANDREJA LESKOVAC, BRANISLAV NASTASIJEVIĆ, VESNA VASIĆ*

Vinča Institute of Nuclear Sciences, University of Belgrade, P.O.Box 522, 11001 Belgrade, Serbia

The spherical gold nanoparticles (NPs) of different average size (15 nm and 47 nm) prepared by citrate reduction were used to examine their cytotoxic effects. UV-vis spectrophotometry, transmission electron microscopy (TEM), dynamic light scattering (DLS) and zeta potential measurements were used to characterize the gold NPs. We have investigated the concentration and size dependent cytotoxic effects of gold NPs, using two *in vitro* human cells model systems: proliferating lymphocytes and connective tissue fibroblasts. Treatment of lymphocyte cultures with Au NPs caused cytotoxic effects as revealed by significant enhancement of incidence of micronuclei but non significant increase of cell proliferation potential when compared to the control. In a fibroblast cell line, the same doses of gold NPs induced the slightly higher level of γ-H2AX foci than in a control. The presented results clearly indicate that the enhancement of micronuclei incidence and proliferation index depend not only on concentration but also the size of the nanoparticles.

(Received August 16, 2011; accepted September 16, 2011)

Keywords: gold, human cells, nanoparticles, cytotoxicity

1. Introduction

The novel properties of metallic nanoparticles, different from those of bulk materials, have stimulated considerable research effort in both their synthesis and application [1-6]. The noble metal NPs (mainly gold) have widely been paid attention due to their current and future applications not only in the field of catalysts but also in the field of biology and medicine [7, 8], such as diagnostics [9], biosensing [10, 11], therapeutics [12, 13], drug delivery and targeting [14-17]. The bio-compatibility of this NPs have been used to deliver antitumor agents at site of the tumor by the enhanced permeability and retention effect [15], and also act as a non-viral-based gene delivery system [18-20]. Research in this area is mainly motivated by the possibility of applications of gold NPs for cancer detection and therapy [21-24].

From the point of view of consumer applications of nanosized materials, the potential long term effects on living organisms must also be taken into account. It is evident that, for any clinical application, biocompatibility of the nanoparticles is crucial. The toxicity of gold nanoparticles inside the biological system has always been an issue of concern. Toxicological studies suggest that nanoparticles may cause adverse health effects, but the fundamental cause-effect relationships are ill defined [25, 26]. However, the impact of gold NPs on human and environmental health remains still unclear [27]. Recent study of the toxicity of gold NPs indicated, that although some precursors of nanoparticles may be toxic, the nanoparticles themselves are not necessarily detrimental to cellular functions [28].

*Corresponding author: evasic@vinca.rs

Generally, gold NPs are considered to be benign, but they were also variously described as nontoxic [28] or toxic [29, 30]. It was found that the increasing toxicity of gold NPs may result from the decreasing their dimensions rather then changing their chemical structure, since very small (1 nm in diameter) can penetrate both the cell and nuclear membranes and become attached to DNA [31]. However, they are similar in size compared to biological matters, such as cellular components and proteins, and the size similarity could lead to undesired cellular entry which might be detrimental to normal cellular function [7]. However, a number of questions remain unanswered for the fate of gold NPs upon their entrance into the living cells. It is now well demonstrated that the main route for the gold NPs entrance into living cells is through the endocytosis [32, 33] and there are several studies indicating size, shape and surface property dependent cellular uptake of gold NPs [29, 34]. The latest studies indicate that the gold NPs mostly remain in the endosomes, spherical double layer of membrane lipids, in the living cells [29, 34]. Due to the fact that the fate of the gold NPs in living cells is not evidently known, there is a need for clear understanding of their destinations and possible interactions with the cell components.

This paper aims to provide additional information in this field of research. Particular attention is paid to investigation of the genotoxicity of gold NPs of different size, surface properties and concentration using two different primary human cells: lymphocytes and fibroblasts. In order to clarify the processes involved we focused on the effects of nanoparticles on individual living cells, and since the skin is the first barrier against exposure to environmental factors containing nanoparticles we chose to study these effects on human dermal fibroblast cells from primary cultures. On the other hand, we chose lymphocytes because their exposure to gold nanoparticles could confirm the direct intracellular penetration effect [35]. Genotoxicity of Au nanoparticles was assessed employing cytokinesis block micronucleus test and γ-H2AX phosphorylation assay.

The *in vitro* micronucleus assay is a mutagenic test system used in toxicological screening for the detection of potential genotoxic compounds which induce the formation of small membrane bound DNA fragments i.e. micronuclei in the cytoplasm of interphase cells. The cytokinesis-block micronucleus assay is very sensitive and simple indicator of chromosome damage, both chromosome loss and chromosome breakage, which also provides information on cell cycle progression and cytotoxicity. By classifying cells according to the number of nuclei, this assay provides an index of cytotoxicity (binucleate cell index, BCI) [36] and information on the cell cycle kinetics (cytokinesis-block proliferation index, CBPI [37]. The purpose of the micronucleus assay is to detect those agents which modify chromosome structure and segregation is such a way as to lead to induction of micronuclei in interphase cells. Genotoxic activity is indicated by a statistically significant, dose-related increase in the incidence of micronuclei the treatment group compared with the concurrent control group.

H2AX is one of several genes coding for histone H2A, which can undergo phosphorylation, acetylation and ubiquitination to regulate the cellular events [38]. Phosphorylation of H2AX is induced in response to DNA double strand breaks (DSBs) originated from diverge origins including external damage, replication fork collision, apoptosis and dysfunctional telomeres [39]. γ-H2AX phosphorylation assay is a technique that has been widely used to quantify the exact amount of DNA double strand breaks (DSBs) in cells produced by radiation and ionizing agents and the repair kinetics.

2. Materials and methods

2.1 Materials

Kalium tetrachloroaurate ($KAuCl_4$, 99%), trisodium citrate dihydrate ($C_6H_5Na_3O_7 \times 2H_20$, 99%), monovalent cation chlorides (KCl, NaCl, LiCl, CsCl), were purchased from Aldrich and used as received. Water purified with a Milipore Milli-Q water system was used for preparing all solutions.

2.2 Synthesis of gold nanoparticles

Gold NPs solutions were prepared by the standard citrate reduction method [40]. Briefly, 200-mL sample of 1 mM $KAuCl_4$ was brought to a vigorous boil with stirring in a round-bottom flask fitted with a reflux condenser. Then, 20 mL or 10 mL of 38.8 mM sodium citrate was rapidly added to the boiling solution to prepare colloid Au-1 and colloid Au-2, respectively. The solution was kept boiling for another 15 min, during which time the solution changed color from pale yellow to deep red (wine-red) and was then allowed to cool down with continued stirring. Citrate acts as both a reducing and a loosely bound capping agent stabilizing the particles. The size of the nanospheres can be controlled by varying the citrate/gold ratio. Generally, smaller amount of citrate will yield larger nanospheres. The final concentrations of gold colloidal solutions were 1.14 mM (Au-1) and 1.19 mM (Au-2).

2.3 Methods

Blood sample was obtained from healthy 30 years old male, non-smoking volunteer in the Medical Unit in accordance with the current Health and Ethical regulations in Serbia [41].

For micronuclei analysis, aliquots of heparinized whole blood (0.5 mL) were set up in cultures containing PBmax-karyotyping medium (Invitrogen-Gibco) in the presence of gold colloids. The micronuclei were prepared according to the method described by Fenech et al [42]. At least 1000 binucleated cells were scored.

The ability of cells to proliferate *in vitro* was evaluated by counting the number of cells with one to four micronuclei on the same slides. The results of these analyses are presented as a cytokinesis-block proliferation index (CBPI). CBPI was calculated as follows: CBPI=MI+2MII+3[MIII+MIV]/N, where MI-MIV represents the number of cells with one to four nuclei, respectively, and N is the number of cells scored [43].

Study on fibroblasts was performed on human fibroblast cell line. Normal human dermal fibroblasts HDMEC (PromoCell) were grown under standard tissue culture conditions in DMEM supplemented with 10% of fetal bovine serum at 37^{o}C and 10% of CO_2. Exponentially growing cells were seeded on polylysine glass-slides (Sigma-Aldrich) and allowed to attach to the slide surface for 24 hours before treatment with increasing doses of Au colloidal nanoparticles Au-1 and Au-2. Repair kinetics of induced DNA double-strand breaks (DSBs) was measured after 24 hours.

For cell immunostaining, cells were fixed in 4% formaldehyde, permeabilised with 0.2% triton X-100 and stained with a phosphospecific primary antibody and FITC-labeled secondary antibody (Sigma, Aldrich). The slides were mounted with 4′, 6'-diamidino-2-phenylindole (DAPI)-containing antifade solution (Vector Laboratories), covered with coverslips and sealed.

Statistical analysis was performed using the statistical software package Statistica 6.0 for Microsoft Windows. Among parameters under consideration, Product-Moment and partial correlations and Student's *t* test were used and a P value < 0.05 was considered to be significant.

2.4 Physical measurements

UV-vis absorption spectra of the colloidal solutions in a quartz cuvette (1 cm optical path length) were measured using a Lambda 35 spectrophotometer (Perkin Elmer).

The diameter and zeta potential of particles were monitored by dynamic light scattering measurements (DLS) at 25^0 C, using a Zetasizer Nano, ZS with 633 nm He-Ne laser, equipped with a MPT-2 Autotitrator (Malvern, UK). Each curve/run presents an average result of 14 measurements.

Transmission electron microscope (TEM, JOEL 100CX) was also used to observe the morphology and average size of Au nanoparticles.

The micronuclei were recorded using an AxioImager A1 microscope (Carl Zeiss, Jena, Germany) with 400× or 1000× magnification. γ-H2AX foci were counted using epifluorescent microscope Axiomager A1 (Carl Zeiss) and the software Image J.

3. Results and discussion

3.1 Physicochemical Characterization of gold NPs

Special attention in our work is devoted to the study of the particle size-dependent effects. To this end, we prepared two gold colloidal dispersions (Au-1, Au-2) with different nanoparticles size. The UV-Vis absorption spectra of these solutions, (Fig.1) show the localized surface plasmon resonance (LSPR) peaks at 523 and 543 nm, for Au-1 and Au-2 colloidal dispersion, respectively. Such intensive absorption of gold nanoparticles arises from the collective oscillations of the free conduction band electrons that are induced by the incident electromagnetic radiation. Their brilliant colors are manifestation of LSPR in the visible region. The expected red-shift of the maximum plasmon peak position for increasing particle diameters could be observed and it was reflected in the change of the sample color from wine-red (Au-1) to purple (Au-2).

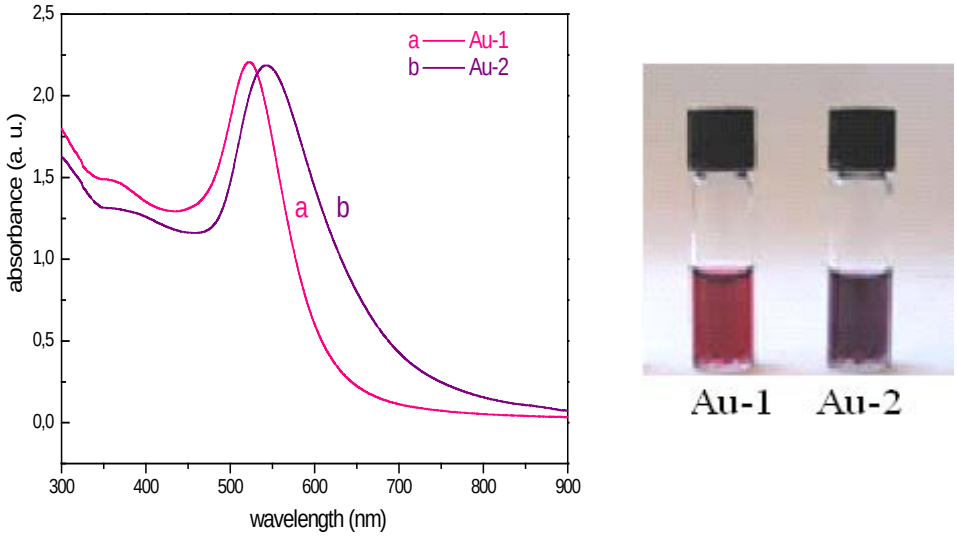

Fig.1 Absorption spectra of gold colloids with different sizes and photographs of these colloidal dispersions: a) Au-1 and b) Au-2 (color of line corresponds to solution color)

The shape and size distribution of the gold nanoparticles were examined by TEM and a representative image of both Au colloidal dispersions and their associated size distributions are shown in Fig.2 and Fig.3. Based on TEM measurements, the gold NPs are nearly spherical in shape with a relatively narrow size distribution. The obtained average particle diameters were 15 nm (Fig.2), and 47 nm (Fig.3) for Au-1 and Au-2 nanoparticles, respectively.

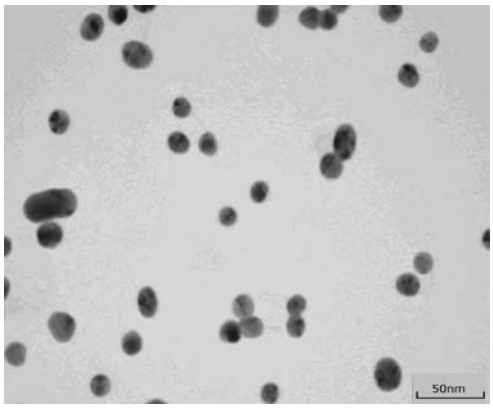

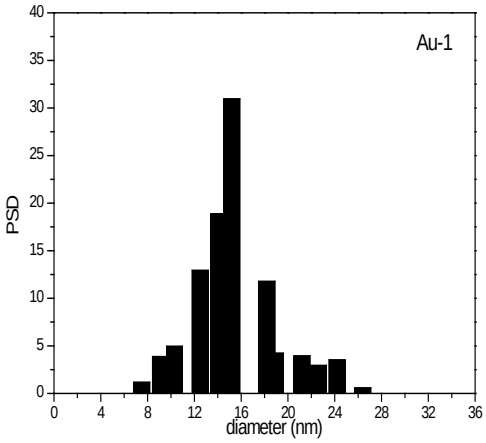

15 nm

Fig. 2 TEM image of the citrate capped Au-1 nanoparticles with the corresponding size distribution histogram based on 200 particles (PSD stands for the particle size distribution)

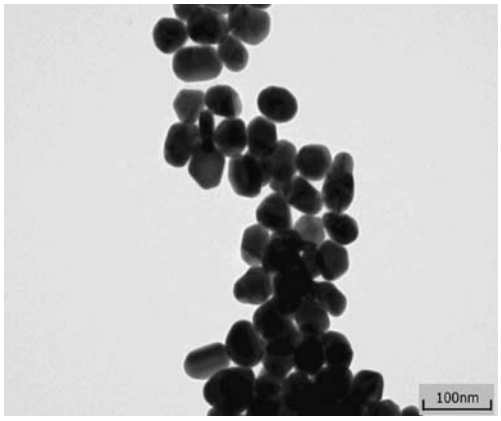

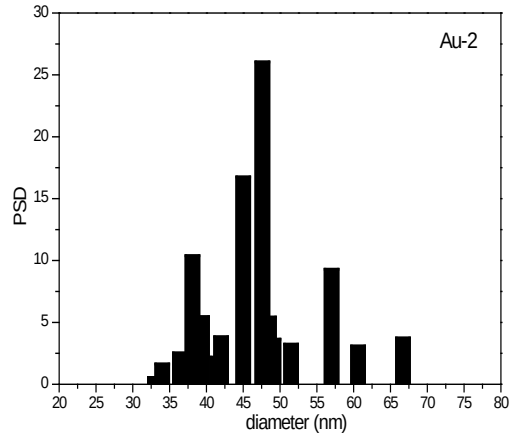

47 nm

Fig. 3 TEM image of the citrate capped Au-2 nanoparticles with the corresponding size distribution histogram based on 200 particles (PSD stands for the particle size distribution)

The particle size distribution (PSD) measurements by DLS method were also performed, using prepared Au colloidal dispersions, seven days after preparation (age time) of the sols. The values of average particle diameter, d_{av}, based on the scattering light intensity, are given in Table 1. The obtained d_{av} values represent the hydrodynamic diameter of a sphere (i.e. diameter of particle with hydratation shell) having the same volume as the particle. The comparison of results obtained by TEM and DLS measurements (Table 1) indicated that particle sizes obtained by TEM were smaller than that obtained by DLS, since the particle size obtained by DLS measurements included the added solvent or stabilizer moving with the particle. In addition, DLS method provides information on the size of aggregates rather than on the diameter of individual nanoparticles, while the TEM measures a number based on size distribution of the physical size only.

In addition, zeta potential for initial Au colloidal dispersions was measured in the lymphocyte culture medium at the end of cell harvesting (pH 8.5), Table 1. It has been well established that gold NPs consist of an elemental gold core surrounded by a negative ionic double layer of charges [44]. These charges are determined by the zeta potential of the particle in each

system. It can be seen that as the amount of negatively charged capping agents increases, the absolute value of the zeta potential increases.

Table 1 The values of average gold NPs diameter and zeta potential in lymphocyte culture medium (pH 8.5)

Colloid	Diameter (nm) from TEM	z-average diameter (nm) by DLS	Polydispersity index (PDI)	Zeta potential (mV)
Au-1	15±2	17.93±0.34	0.300±0.030	-41.9±1.27
Au-2	47±2	49.44±2.76	0.334±0.062	-38.0±0.778

3.2 Influence of colloid particles on the cell cultures

Lymphocyte cultures were treated with different doses of colloid suspensions, containing from 1 to 20 µg/ mL gold in final volume for cell culture medium. The results obtained for lymphocytes exposed to increasing concentrations of gold colloids Au-1 and Au-2 (µg/mL) are presented in Table 2.

Table 2 Incidence of micronuclei and cytokinesis-block proliferation index in lymphocyte cultures treated with Au colloidal nanoparticles Au-2 (47 nm) and Au-1 (15 nm).

Concentration of Au colloid (µg / mL Au)	Incidence of micronuclei MN/1000 BN	Distribution of micronuclei No. of binucleated cells (BN) with 0	1	2	3	4	5	CBPI
Untreated control	24.46	1080	21	3				1.75
Au-2 (47 nm)								
1.8	45.62	1050	44		2			1.80
3.6	49.38	1710	56	16				1.84
11.1	51.65	1386	57	9				1.85
14.5	88.89	1248	86	14	2			1.87
16.5	85.71	1044	64	8		4		1.97
18.2	83.74	1146	54	6	12			1.93
Au-1 (15 nm)								
1.8	73.73	1015	60	10				1.84
3.6	77.70	1098	82	2	2			1.82
11.1	79.66	1320	64	20		2		1.99
14.5	90.09	1634	128	10	4			1.93
16.5	102.76	1474	94	20	4	2	2	1.90
18.2	65.10	1089	51	12				1.85

Treatment of lymphocyte cultures with gold colloids Au-1 and Au-2 caused cytotoxic effects as revealed by significant enhancement of incidence of micronuclei and non significant increase of cell proliferation potential when compared to the control ($p < 0.05$). The citrate capped nanoparticles induced the MN formation in harvested human lymphocytes up to 350% above the control value for Au-2, and up to 420% above the control value for Au-1, and with further increasing of gold concentration, the incidence of MN decreased. It is worthily to notice that the effect is rather stronger for smaller particles (colloid Au-1) in the presence of the same amount of Au. For example, when the concentration of both Au colloids is 1.8 µg/mL, the incidence of micronuclei (MN/1000 BN) in the case of Au-1 is 73.73 and in the case of Au-2 is 45.62 (Table 2). The possible explanation for this is a that a different number of nanopaticles is involved, namely in the case of Au-1 the number of nanoparticles (for this same amount of Au) is 5.3×10^{13} and for Au-2 is 1.7×10^{12}, meaninig that there are more particles of Au-1 colloid which can make a stronger

influence than in the case of Au-2. This fact, together with different cellular uptake could be the reason for differences in toxicity for these two colloids.

Moreover, proliferation potential of cells was in correlation with the above described results, i.e. the effect of gold nanoparticels on micronuclei incidence was followed by the small increase of cell proliferation, which was statistically non significant. However, CBPI increased ($p < 0.05$) in a dose-dependent manner compared to the control, until achieved the maximum value.

The obtained results clearly suggest, that the incidence of micronuclei and cytokinesis-block proliferation index correlated positively, at the border of statistical significance ($p = 0.06$). Generally, treatment of lymphocyte cultures with Au-1 colloid (15 nm) induced higher cytotoxic effects than that observed in treatments with Au-2 colloid (47 nm).

In addition, the incidences of γ-H2AX foci in fibroblasts treated with Au nanoparticles Au-1 and Au-2 was tested. When applied on monolayer fibroblast cells, citrate capped gold nanoparticles induced DSBs in a dose dependent manner (Table 3). However, the incidences of γ-H2AX foci were slightly increased compared to that in untreated control, with no statistical significance ($p > 0.05$). Although comparable results could be seen in both studied cell systems, the nonsignificant increase of the DSBs in fibroblasts treated with gold colloids suggest that micronuclei in lymphocytes originated prevalently from chromosome loss, and at minor extant, from chromosomal fragmentation indicating that gold nanoparticles do not display clastogenic mode of action. Enhancement of cell proliferation in the presence of Au particles, which is followed with increased number of micronuclei, suggested that Au particles disturb cell cycle control checkpoints, enabling uncontrolled proliferation and entering in mitosis with unrepaired genomic damages, typical for the phenomenon of mitotic catastrophe. Genotoxic properties of Au nanoparticles observed in this study are unique and should be further investigated.

Table 3 Incidence of γ-H2AX foci in human fibroblast cell line treated with Au colloidal nanoparticles Au-1 and Au-2

Concentration of Au colloid (μg/mL Au)	Number of cells analyzed	Incidence of γ-H2AX foci per cell
Untreated control	340	3.56
Au-2 (47 nm)		
1.8	335	3.60
3.6	341	3.64
11.1	338	3.62
14.5	300	3.77
16.5	324	3.81
18.2	280	3.88
Au-1 (15 nm)		
1.8	328	3.77
3.6	330	3.91
11.1	335	3.87
14.5	318	3.90
16.5	294	4.11
18.2	275	4.08

It was further of interest to represent the obtained results as the function of nanoparticle size and concentration. Assuming that gold nanoparticles were spherical in shape, we used the following form $C_{NPs} = C/n$ to calculate the concentration of nanoparticles (C_{NPs}) in the colloid concentration C. The aggregation number n is defined as follows

$$n = \frac{\pi \cdot \rho \cdot N_A \cdot d^3}{6 \cdot M} \quad (1)$$

where ρ is the density for gold (19.3 g/cm^3), d is the particle diameter, N_A is the Avogadro's constant and M stands for atomic weight of gold (196.97 g/mol). The calculated values of nanoparticles concentration were 1.1×10^{-8} M (Au-1) and 3.7×10^{-10} M (Au-2), assuming that the reduction from gold(III) to gold atoms was 100% complete.

The dependence of the incidence of MN and CPBI on the nanoparticle concentration is presented in Fig.4. The presented results clearly indicate that the enhancement of the micronuclei incidence and proliferation index depend not only on concentration but also the size of the nanoparticles. Moreover, the nanoparticles with the largest diameter (47 nm) enhanced the incidence of MN and CPBI at lower concentrations then the smaller nanoparticles (15 nm).

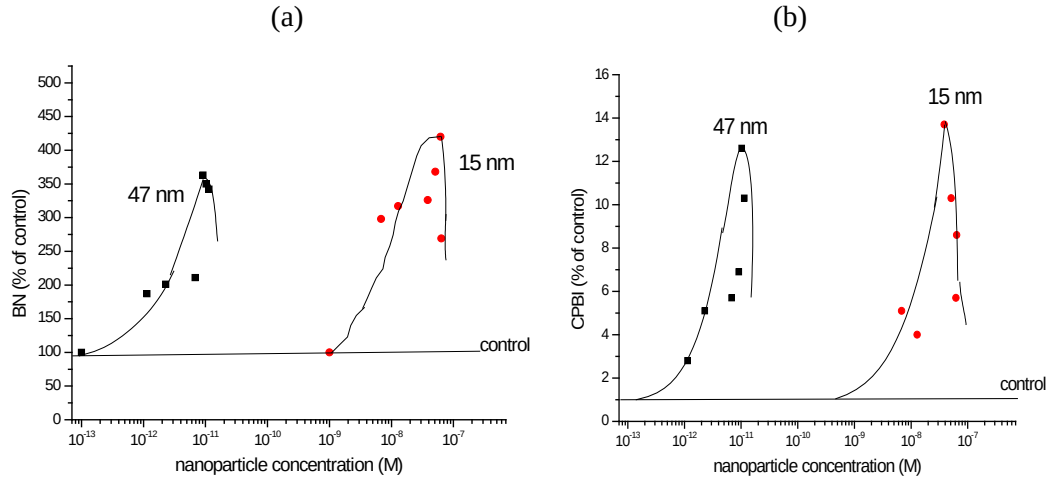

Fig. 4 Dependence of incidence of micronuclei (a) and proliferation index (b) (presented as percentage of control) on the nanoparticle concentration in lymphocyte cultures treated with gold colloids of various particle size

However, the interaction of nanoparticles and cells depends also on the nanoparticle charge [45]. The size and charge of nanoparticles may affect *in vitro* cellular uptake. Since Au nanoparticles are negatively charged (similar values of negative zeta potential for both colloids were obtained), they possess strong properties for capturing the oppositely charged species in solution through electrostatic interactions and their genotoxic properties in some extent can be attributed to their electrochemical properties. However, the most interesting finding is that genotoxic effects are due to disturbances of cell-cycle control checkpoints, which have physiological role to verify whether the processes at each phase of the cell cycle have been accurately completed before progression into the next phase. Two major checkpoints have been identified, Chk1 and Chk2. The function of these checkpoints is to assess DNA damage, which is detected by sensor mechanisms. The most sensitive sensors of the DNA damage is γ-H2AX assay [46], which showed almost no induction of DSBs during treatment with Au nanoparticles (Fig. 5). However, on lymphocyte cells system where cells were growing more rapidly, a huge amount of unrepaired damages that resulted in MN were found indicating that cells have no ability to stall the cell cycle until repairs are made. Cell cycle progression is tightly regulated by cyclins, cyclin-dependent kinases (CDKs), cyclin-dependent kinase inhibitors (CKIs), and the tumor suppressor proteins such as p53 and the retinoblastoma susceptibility gene product (pRb) [47]. Although further investigations are warranted to assess the molecular mechanisms that result in cell cycle promotion, we hypothesize that gold nanoparticles stimulate proliferation of lymphocytes by altering the expression and/or function of the above proteins. Given our findings, a more comprehensive assessment is needed to provide important information for the future safe applications and the design of more biocompatible nanomaterials.

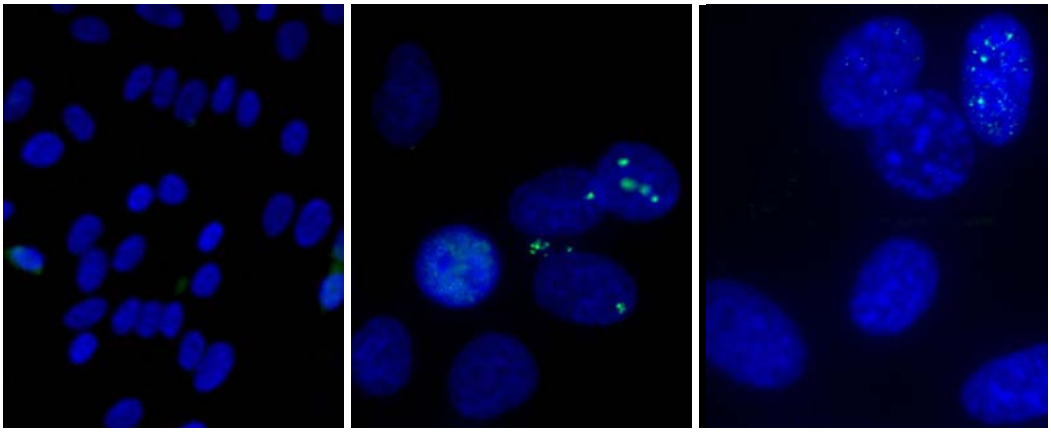

Fig. 5 γ-H2AX foci induced by Au nanoparticles (green spots)

4. Conclusions

In conclusion, our investigations were performed on two *in vitro* human cells model systems: proliferating lymphocytes and connective tissue fibroblast. The obtained results showed the concentration dependent effects in both cases, although lymphocytes turned to be more sensitive to gold nanoparticles. Treatment of lymphocyte cultures with gold colloids caused cytotoxic effects as revealed by significant enhancement of incidence of micronuclei but non significant increase of cell proliferation potential when compared to the control, still suggesting disturbed function of cell-cycle checkpoints. These results clearly indicate that the enhancement of micronuclei incidence and proliferation index depend not only on concentration but also the size of the nanoparticles. We propose these methods and cell systems as very good model systems for evaluation of genotoxicity.

Acknowledgment

Authors would like to thank to the Ministry of Science and Technological Development of the Republic of Serbia (Project No. 172023) for their financial support.

References

[1] M. C. Daniel, D. Astruc, Chem. Rev. **104**, 293 (2004).
[2] M. Brust, C. J. Kiely, Colloids Surf., A **202**, 175 (2002).
[3] M. A. El-Sayed, Acc. Chem. Res. **34**, 257 (2001).
[4] S. Sun, C. B. Murray, J. Appl. Phys. **85**, 4325 (1999).
[5] S. Underwood, P. Mulvaney, Langmuir **10**, 3427 (1994).
[6] W. Wang, S. Efrima, O. Regev, Langmuir **14**, 602 (1998).
[7] P. C. Chen, S. C. Mwakwari, A. K. Oyelere, Nanotechnology **1**, 45 (2008).
[8] C. Pranjal, D. Debasmita, A. A. Adel, Dig. J. Nanomater. Bios. **5**, 363 (2010).
[9] S. K. Sahoo, S. Parveen, J. J. Panda, Nanomedicine **3**, 20 (2007).
[10] Y. Li, H. J. Schluesener, S. Xu, Gold Bull. **43**, 29 (2010).
[11] L. Olofsson et al., Langmuir **19**, 10414 (2003).
[12] D. M. Leander, C. S. Thaxton, A. J. Luthi, Nanoscape **7**, 11 (2010).
[13] A. C. Powell, G. F. Paciotti, S. K. Libutti, Methods Mol. Biol. **624**, 375 (2010).
[14] W. H. De Jong, P. J. Borm, Int. J. Nanomed. **3**, 133 (2008).
[15] G. F. Paciotti et al., Drug Deliv. **11**, 169 (2004).
[16] D. Kim et al., J. Am. Chem. Soc. **129**, 7661 (2007).

[17] G. Sonavane, K. Tomoda, K. Makino, Colloids Surf. B **66**, 274 (2008).
[18] M. Thomas, A. M. Klibanov, Proceedings of the National Academy of Sciences of the United States of America **99**, 14640 (2002).
[19] J. Panyam, V. Labhasetwar, Adv. Drug Deliver. Rev. **55**, 329 (2003).
[20] P.-H. Yang et al., Bioconjugate Chem. **16**, 494 (2005).
[21] P. K. Jain, I. H. El-Sayed, M. A. El-Sayed, Nano Today **2**, 18 (2007).
[22] J. F. Hainfeld, D. N. Slatkin, H. M. Smilowitz, AACR Meeting Abstracts **2005**, 287 (2005).
[23] X. Huang et al., J. Am. Chem. Soc. **128**, 2115 (2006).
[24] C. Loo et al., Technol. Cancer Res. T. **3**, 33 (2004).
[25] C. J. Murphy et al., Acc. Chem. Res. **41**, 1721 (2008).
[26] Y. Pan et al., Small **3**, 1941 (2007).
[27] A. M. Alkilany, C. J. Murphy, J. Nanopart. Res. **12**, 2313 (2010).
[28] E. E. Connor et al., Small **1**, 325 (2005).
[29] C. M. Goodman et al., Bioconjugate Chem. **15**, 897 (2004).
[30] N. Pernodet et al., Small **2**, 766 (2006).
[31] M. Tsoli et al., Small **1**, 841 (2005).
[32] R. Shukla et al., Langmuir **21**, 10644 (2005).
[33] E. J. Andreu et al., J. Histochem. Cytochem. **46**, 1199 (1998).
[34] S. Hoffmann et al., Nano Lett. **6**, 622 (2006).
[35] V. Wiwanitkit, A. Sereemaspun, R. Rojanathanes, Turk. J. Hematol. **26**, 29 (2009.).
[36] M. Fenech, Environ. Health Perspect. **101**, 101 (1993).
[37] M. Kirsch-Volders et al., Mutat. Res. **540**, 153 (2003).
[38] E. P. Rogakou et al., J. Biol. Chem. **273**, 5858 (1998).
[39] K. Rothkamm, M. Lobrich, Mutat. Res. **433**, 193 (1999).
[40] K. Grabar et al., Anal. Chem. **67**, 735 (1995).
[41] Parliament of the Republic of Serbia **107**, 112 (2005).
[42] M. Fenech, Mutat. Res. **285**, 35 (1993).
[43] J. Surralles et al., Mutat. Res. **342**, 43 (1995).
[44] G. Frens, Nature Phys. Sci. **241**, 20 (1973).
[45] L. Liu et al., Nat. Nanotechnol. **4**, 457 (2009).
[46] G. P. Watters et al., Mutat. Res., Gen. Tox. En. **679**, 50 (2009).
[47] D. M. Huang et al., Biomaterials **30**, 3645 (2009).